

1

# NATIONAL ADVISORY COMMITTEE FOR AERONAUTICS

TECHNICAL NOTE

No. 1671

Ref 17

EFFECT OF TAPER RATIO ON LOW-SPEED STATIC AND YAWING  
STABILITY DERIVATIVES OF  $45^\circ$  SWEPTBACK WINGS

WITH ASPECT RATIO OF 2.61

By William Letko and John W. Cowan

Langley Aeronautical Laboratory  
Langley Field, Va.



Washington  
July 1948

# NATIONAL ADVISORY COMMITTEE FOR AERONAUTICS

TECHNICAL NOTE NO. 1671

## EFFECT OF TAPER RATIO ON LOW-SPEED STATIC AND YAWING STABILITY DERIVATIVES OF $45^\circ$ SWEEPBACK WINGS WITH ASPECT RATIO OF 2.61

By William Letko and John W. Cowan

### SUMMARY

A low-speed wind-tunnel investigation was made to determine the effect of taper ratio on the static and yawing stability derivatives of three tapered wings each with a constant sweepback of  $45^\circ$  at the quarter-chord line and with an aspect ratio of 2.61. The wings were of the NACA 0012 airfoil section in planes perpendicular to the quarter-chord line. The wings had taper ratios of 1.00, 0.50, and 0.25.

The results of the tests in straight flow indicated that the lift-curve slope at low and moderate lift coefficients was almost unaffected by changes in taper ratio. The aerodynamic center at low lift coefficients shifted rearward 11 percent of the mean aerodynamic chord with a decrease in taper ratio from 1.00 to 0.25. For low and moderate lift coefficients, the rate of change of effective dihedral with lift coefficient decreased as the wing taper ratio decreased.

The results of the tests in yawing flow indicated that the rate of change of rolling moment due to yawing with lift coefficient decreased as the wing taper ratio decreased. The change in taper ratio had little effect on the yawing moment due to yawing.

In general, the trends in the characteristics resulting from effects of taper were indicated with fair accuracy by the available theory.

### INTRODUCTION

Estimation of the dynamic flight characteristics of airplanes requires a knowledge of the component forces and moments resulting from the orientation of the airplane with respect to the air stream and from the rate of angular motion of the airplane about each of its axes. The forces and moments resulting from the orientation of the airplane normally are expressed as the static stability derivatives, which are readily determined from conventional wind-tunnel tests. The forces and moments resulting from the angular motions (rotary derivatives) have generally been estimated from theory because of the lack of a convenient experimental technique.

The recent application of the rolling-flow and curved-flow principle in the Langley stability tunnel has made possible the determination of both rotary and static stability derivatives with about the same ease. Preliminary tests (data obtained in the Langley stability tunnel) have indicated that although the rotary stability derivatives of unswept wings of moderate or high aspect ratio can be predicted quite accurately from the available theory, the use of sweep and, perhaps, low aspect ratio introduces effects which are not readily amenable to theoretical treatment. For this reason, a systematic research program has been established for the purpose of determining the effects of various geometric variables on both rotary and static stability characteristics.

This paper presents the results of an investigation made to determine the effect of taper ratio on the static and yawing stability derivatives of three tapered wings each with a constant sweepback of  $45^\circ$  at the quarter-chord line and with an aspect ratio of 2.61. The experimental results are compared with theory.

#### SYMBOLS

The data are presented in the form of standard NACA coefficients of forces and moments which are referred, in all cases, to the stability axes with the origin at the quarter-chord point of the mean aerodynamic chord of the models tested. The positive directions of the forces, moments, and angular displacements are shown in figure 1. The coefficients and symbols used herein are defined as follows:

$C_L$	lift coefficient ( $L/qS$ )
$C_X$	longitudinal-force coefficient ( $X/qS$ )
$C_D$	drag coefficient ( $-C_X$ for $\psi = 0^\circ$ )
$C_Y$	lateral-force coefficient ( $Y/qS$ )
$C_l$	rolling-moment coefficient ( $L'/qSb$ )
$C_m$	pitching-moment coefficient ( $M/qS\bar{c}$ )
$C_n$	yawing-moment coefficient ( $N/qSb$ )
$L$	lift
$X$	longitudinal force
$Y$	lateral force
$L'$	rolling moment about X-axis

M	pitching moment about Y-axis
N	yawing moment about Z-axis
q	dynamic pressure $\left(\frac{1}{2}\rho V^2\right)$
$\rho$	mass density of air
V	free-stream velocity
S	wing area
b	span of wing measured perpendicular to axis of symmetry
c	chord of wing, measured parallel to axis of symmetry
$\bar{c}$	mean aerodynamic chord $\left(\frac{2}{S} \int_0^{b/2} c^2 dy\right)$
y	distance measured perpendicular to the axis of symmetry
x	distance of quarter-chord point of any chordwise section from leading edge of root section
$\bar{x}$	distance from leading edge of root chord to quarter chord of mean aerodynamic chord $\left(\frac{2}{S} \int_0^{b/2} cx dy\right)$
A	aspect ratio $(b^2/S)$
$\lambda$	taper ratio (Tip chord/Root chord)
$\alpha$	angle of attack measured in plane of symmetry, degrees
$\psi$	angle of yaw, degrees
$\Lambda$	angle of sweep, degrees
$rb/2V$	yawing-velocity parameter
r	yawing angular velocity, radians per second
$C_{L_\alpha}$	$= \frac{\partial C_L}{\partial \alpha}$
$C_{l_\psi}$	$= \frac{\partial C_l}{\partial \psi}$
$C_{n_\psi}$	$= \frac{\partial C_n}{\partial \psi}$

$$C_{Y\psi} = \frac{\partial C_Y}{\partial \psi}$$

$$C_{l_r} = \frac{\partial C_l}{\partial \frac{rb}{2V}}$$

$$C_{n_r} = \frac{\partial C_n}{\partial \frac{rb}{2V}}$$

$$C_{Y_r} = \frac{\partial C_Y}{\partial \frac{rb}{2V}}$$

#### APPARATUS AND TESTS

The tests reported herein were conducted in the 6- by 6-foot test section of the Langley stability tunnel. In this test section, curved flight is approximately simulated by causing the air to flow in a curved path about a fixed model.

The models tested were three wings of NACA 0012 airfoil section in planes perpendicular to the quarter-chord line. The wings had taper ratios of 1.00, 0.50, and 0.25. For details of these wings, see figures 2 and 3. In the present tests, the models were mounted rigidly on a single support strut at the quarter-chord point of the mean aerodynamic chord of the model. The forces and moments were measured by means of electrical strain gages mounted on the strut.

All the tests were made at a dynamic pressure of 24.9 pounds per square foot, which corresponds to a Mach number of 0.13. The test Reynolds numbers based on the mean aerodynamic chord of the models varied from about 1,100,000 for the wing with a taper ratio of 1.00 to 1,230,000 for the wing with a taper ratio of 0.25.

The characteristics of the wings were determined in both straight and yawing flow. In the straight-flow tests, six-component measurements were made for each wing through an angle-of-attack range from about  $-4^\circ$  up to and past the angle of maximum lift, at angles of yaw of  $0^\circ$  and  $\pm 5^\circ$ . The tests in yawing flow were made at an angle of yaw of  $0^\circ$  and for four different wall curvatures corresponding to the values of  $rb/2V$  of 0, -0.0316, -0.0670, and -0.0883. In the yawing-flow tests each model was tested through an angle-of-attack range from about  $-4^\circ$  up to and past the angle for maximum lift coefficient.

## CORRECTIONS

Approximate corrections, based on unswept-wing theory, for the effects of the jet boundaries have been applied to the angle of attack, the longitudinal-force coefficient, and the rolling-moment coefficient. The lateral-force and yawing-moment coefficients have been corrected for the buoyancy effect of the static-pressure gradient associated with curved flow.

The values of  $C_{l_r}$  have been corrected for the tare associated with the induced load resulting from the presence of the strut for the wing at an angle of attack of  $0^\circ$ . The same correction was applied throughout the angle-of-attack range.

No other tare corrections have been applied to the data. Corrections for the effects of blocking, turbulence or for the effects of static pressure gradient on the boundary-layer flow have not been applied to these results.

## RESULTS AND DISCUSSION

## Characteristics in Straight Flow

For the range of taper ratio investigated, the change in taper ratio had little effect on the longitudinal-force coefficients at low and moderate lift coefficients. At high lift coefficients, higher longitudinal-force coefficients were obtained with the wings of decreased taper ratio (fig. 4), probably because of more severe tip stalling. Calculations (reference 1) have indicated that the induced drag of sweptback wings is not greatly different from the induced drag of elliptic unswept wings. The increment of drag that is not associated with lift is, therefore, approximately  $C_D - \frac{C_L^2}{\pi A}$ . Curves of  $C_D - \frac{C_L^2}{\pi A}$  plotted against  $C_L$  for the three wings considered in the present investigation are shown in figure 5. The rapid rise in the curves above a lift coefficient of about 0.6 indicates the presence of flow separation from certain parts of the wing. Large changes in some aerodynamic characteristics may occur when separation begins, as is indicated by the increase in the value of drag increment  $C_D - \frac{C_L^2}{\pi A}$ .

At a lift coefficient of about 0.6, all the wings showed an increase in the lift-curve slope, but the increase became smaller as the taper ratio decreased. (See fig. 4.) At lift coefficients less than 0.6, change in taper ratio had very little effect on the lift-curve slope. As can be seen from figure 6, the trend of the slopes obtained experimentally

for this range of lift coefficients is not in agreement with the trend in  $C_{L\alpha}$  predicted for taper by the Weissinger theory and presented in reference 2.

Decrease in taper ratio had little effect on the maximum lift coefficient; however, the angle of attack for maximum lift coefficient is increased with a decrease in taper ratio.

The effect of taper ratio on the pitching-moment coefficients can be seen in figure 4. The position of the aerodynamic center for each wing was computed from these data for lift coefficients up to 0.6 and the data are presented in figure 6 together with the theoretical variation of the position of the aerodynamic center with taper ratio as obtained from reference 2. The experimental data indicate a rearward shift (equal to about 11 percent of the M.A.C.) of the aerodynamic center as the taper ratio is decreased from 1.00 to 0.25. This movement is in fair agreement with theory; however, the experimental data in each case indicate a more rearward position of the aerodynamic center than that predicted by theory. For the wing with taper ratio of 1.00 (see fig. 4), a rearward shift in the aerodynamic center of about 11 percent mean aerodynamic chord occurs at a lift coefficient of about 0.6 (lift coefficient at which the drag increment  $C_D - \frac{C_L^2}{\pi A}$  starts to rise). Only a small shift in aerodynamic center occurred at this lift coefficient for the wing with taper ratio of 0.50 and almost no shift for the wing with taper ratio of 0.25. Some changes in aerodynamic-center position, therefore, can probably be avoided through the proper choice of taper ratio. For these tests the stabilizing shift of the aerodynamic center encountered above a lift coefficient of 0.6 for the wing with taper ratio of 1.00 was minimized by decreasing the taper ratio.

The effect of taper ratio on the static lateral-stability derivatives can be seen in figure 7. The values of  $C_{l\psi}$  increased almost linearly but at slightly different rates with lift coefficient for each wing tested and reached a maximum at a lift coefficient of about 0.6. The maximum value of  $C_{l\psi}$  obtained decreased with a decrease in taper ratio, probably because the tip-stalling tendencies of sweptback wings are aggravated by a reduction in taper ratio.

For low and moderate lift coefficients, the rate of change of effective dihedral  $C_{l\psi}$  with lift coefficient  $C_L$  decreased with a decrease in taper ratio  $\lambda$  and this variation is shown in figure 8, which is a plot of  $C_{l\psi}/C_L$  against  $\lambda$ . The value of  $C_{l\psi}/C_L$  at taper ratio of 0 was obtained from reference 3 for a triangular-plan-form wing of NACA 0012 airfoil section having an aspect ratio of 3. The quarter-chord line of this wing was sweptback  $45^\circ$ . Although the aspect ratio for this wing was slightly higher than that of the other wings reported herein, it is believed that the value of  $C_{l\psi}/C_L$  for the wing with taper ratio of 0 would not be altered enough to make an appreciable difference in the variation shown.

For comparison, the theoretical variation of  $C_{l\psi}/C_L$  with  $\lambda$  for 45° sweptback wings is also shown in figure 8. The theoretical variation was determined by the methods presented in reference 4. Although these values of  $C_{l\psi}/C_L$  are lower than the test values, the decrease in the values with a decrease in taper ratio is similar to the test results.

The previous discussion dealt with the variation of  $C_{l\psi}/C_L$  at lift coefficients below 0.6. Beyond a lift coefficient of about 0.6 (see fig. 7), the values of  $C_{l\psi}$  deviated from their original linear trend and the values of  $C_{l\psi}$  decreased rapidly with an increase in lift coefficient. The deviations of the experimental data from the initial slopes probably results from tip stalling, an indication of which, as was pointed out before, may be the increase in the quantity  $C_D - \frac{C_L^2}{\pi A}$  that results with an increase in lift coefficient. Any variations in test conditions, such as an increase in Reynolds number, that might cause the quantity  $C_D - \frac{C_L^2}{\pi A}$  to increase rapidly at a higher lift coefficient probably would also cause the derivative  $C_{l\psi}$  to maintain its initial linear trend to a higher lift coefficient.

The effect of taper ratio on the values of  $C_{n\psi}$  and  $C_{y\psi}$  is small and is probably unimportant.

#### Characteristics in Yawing Flow

The rate of change of rolling moment due to yawing  $C_{l_r}$  with lift coefficient  $C_L$  generally decreased slightly with a decrease in taper ratio  $\lambda$ . (See fig. 9.) At a lift coefficient of about 0.6 (lift coefficient at which the drag increment  $C_D - \frac{C_L^2}{\pi A}$  starts to rise) the variation of  $C_{l_r}$  with  $C_L$  shows an abrupt change from the initial linearity.

The test values of  $C_{l_r}/C_L$  are compared in figure 10 with theoretical results computed by the methods of reference 4. The test values show a trend with taper ratio similar to that predicted by theory but in each case the test points are higher than the theoretical values.

The change in taper ratio has very little effect on the values of  $C_{n_r}$  at low and moderate lift coefficients as can be seen in figure 9. The theoretical values of  $C_{n_r}$  are compared with test data in figure 11 and the agreement is good except at lift coefficients at or near the stall.

The values of  $C_{y_r}$  become more positive with a decrease in taper ratio. (See fig. 9.) This change, however, is probably of little significance with regard to airplane stability.



## CONCLUSIONS

The results of a low-speed wind-tunnel investigation made to determine the effect of taper ratio on the static and yawing stability derivatives of three tapered wings each with a constant sweepback of  $45^\circ$  at the quarter-chord line and with an aspect ratio of 2.61 indicated the following conclusions:

1. In general, the trends in the characteristics resulting from effects of taper ratio were indicated with fair accuracy by the available theory.

For tests in straight flow:

2. The lift-curve slope was almost unaffected by changes in taper ratio at low and moderate lift coefficients.

3. The aerodynamic center at low lift coefficients shifted rearward 11 percent of the mean aerodynamic chord with a change in taper ratio from 1.00 to 0.25.

4. For low and moderate lift coefficients, the rate of change of effective dihedral with lift-coefficient decreased with a decrease in taper ratio.

For tests in yawing flow:

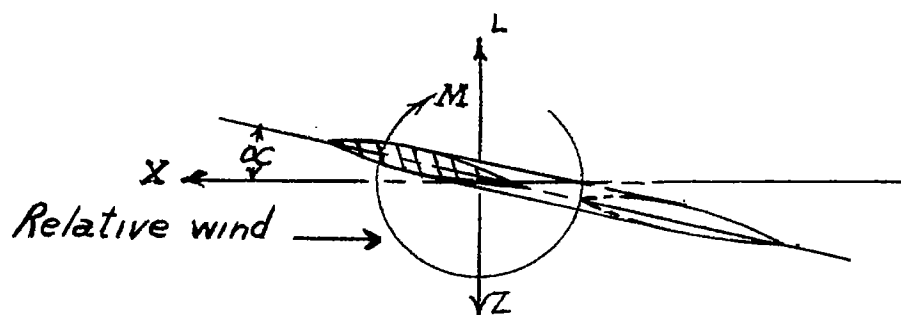
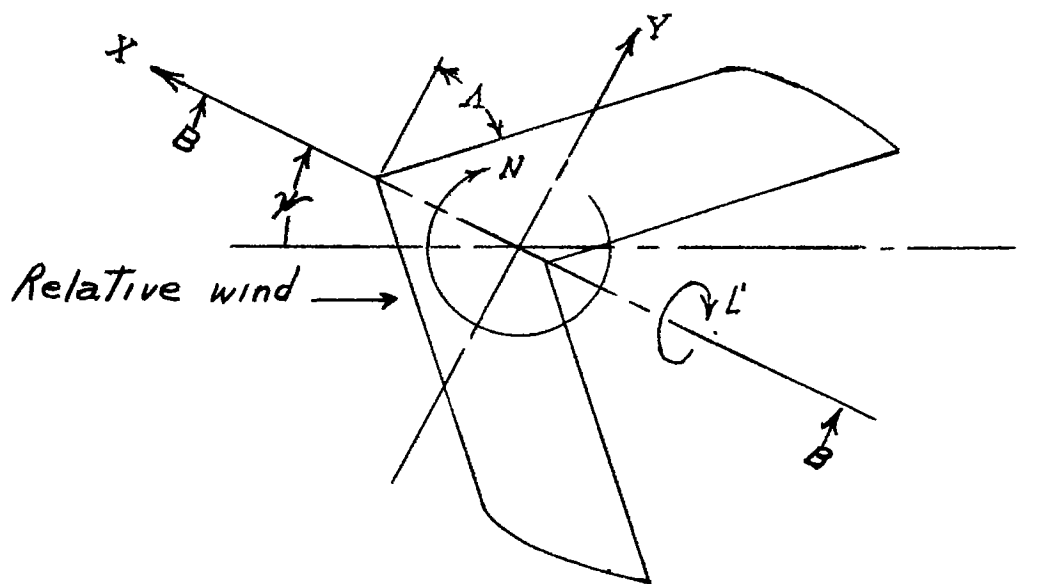
5. The rate of change of rolling moment due to yawing with lift coefficient decreased with a decrease in taper ratio.

6. The change in taper ratio had little effect on the yawing moment due to yawing.

Langley Memorial Aeronautical Laboratory  
National Advisory Committee for Aeronautics  
Langley Field, Va., May 6, 1948

## REFERENCES

1. Mutterperl, William: The Calculation of Span Load Distributions on Swept-Back Wings. NACA TN No. 834, 1941.
2. DeYoung, John: Theoretical Additional Span Loading Characteristics of Wings with Arbitrary Sweep, Aspect Ratio, and Taper Ratio. NACA TN No. 1491, 1947.
3. Lange and Wacke: Test Report on Three- and Six-Component Measurements on a Series of Tapered Wings of Small Aspect Ratio (Partial Report: Triangular Wing). NACA TM No. 1176, 1948.
4. Toll, Thomas A., and Queijo, M. J.: Approximate Relations and Charts for Low-Speed Stability Derivatives of Swept Wings. NACA TN No. 1581, 1948.



### Section B-B

Figure 1.- System of axes used. Positive directions of forces, moments, and angles are indicated.



Figure 2.- Photograph of wing having taper ratio of 0.25 mounted in curved-flow test section of Langley stability tunnel.



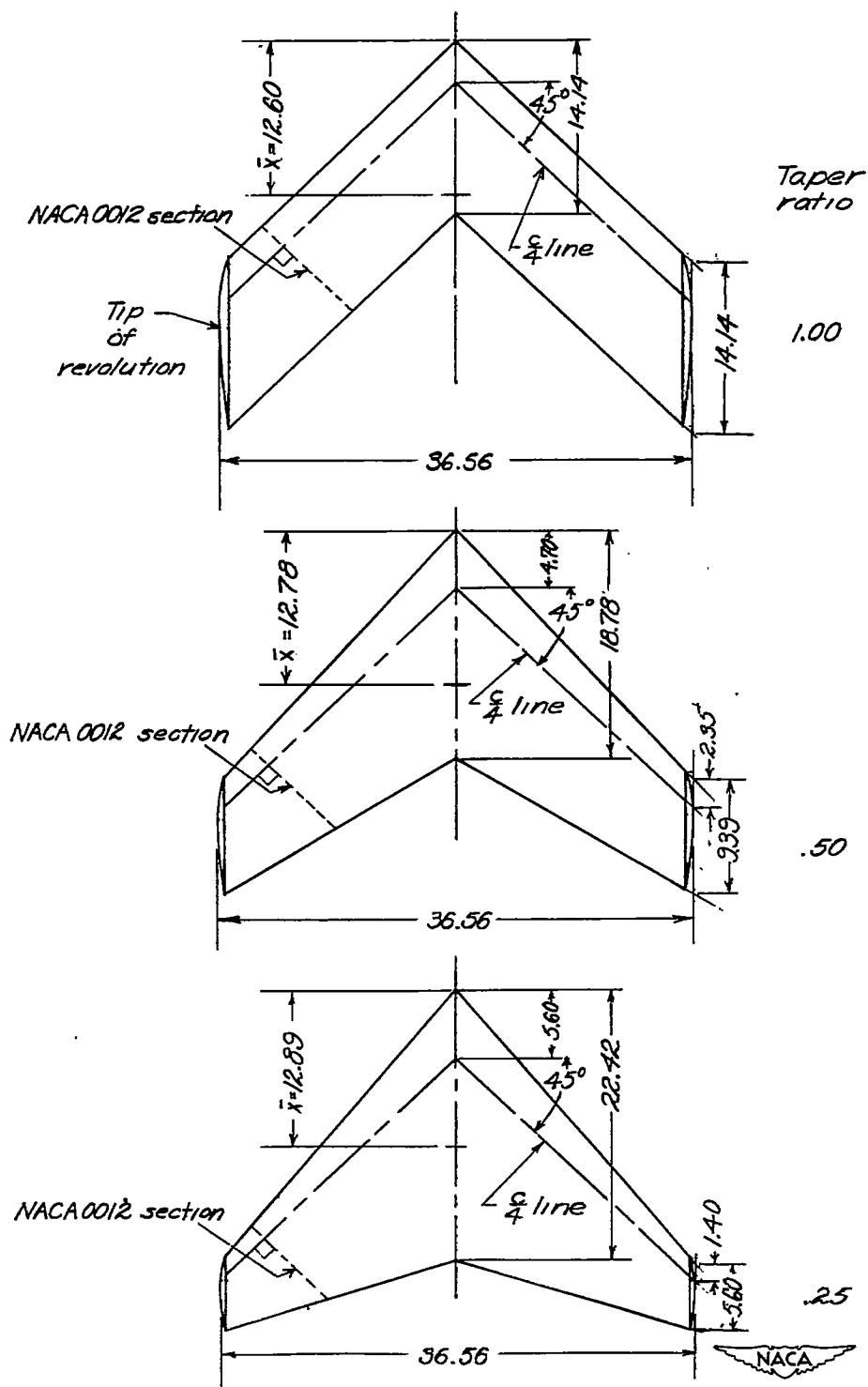


Figure 3.- Plan forms and dimensions of tapered wings tested in Langley stability tunnel. (All dimensions are in inches.)

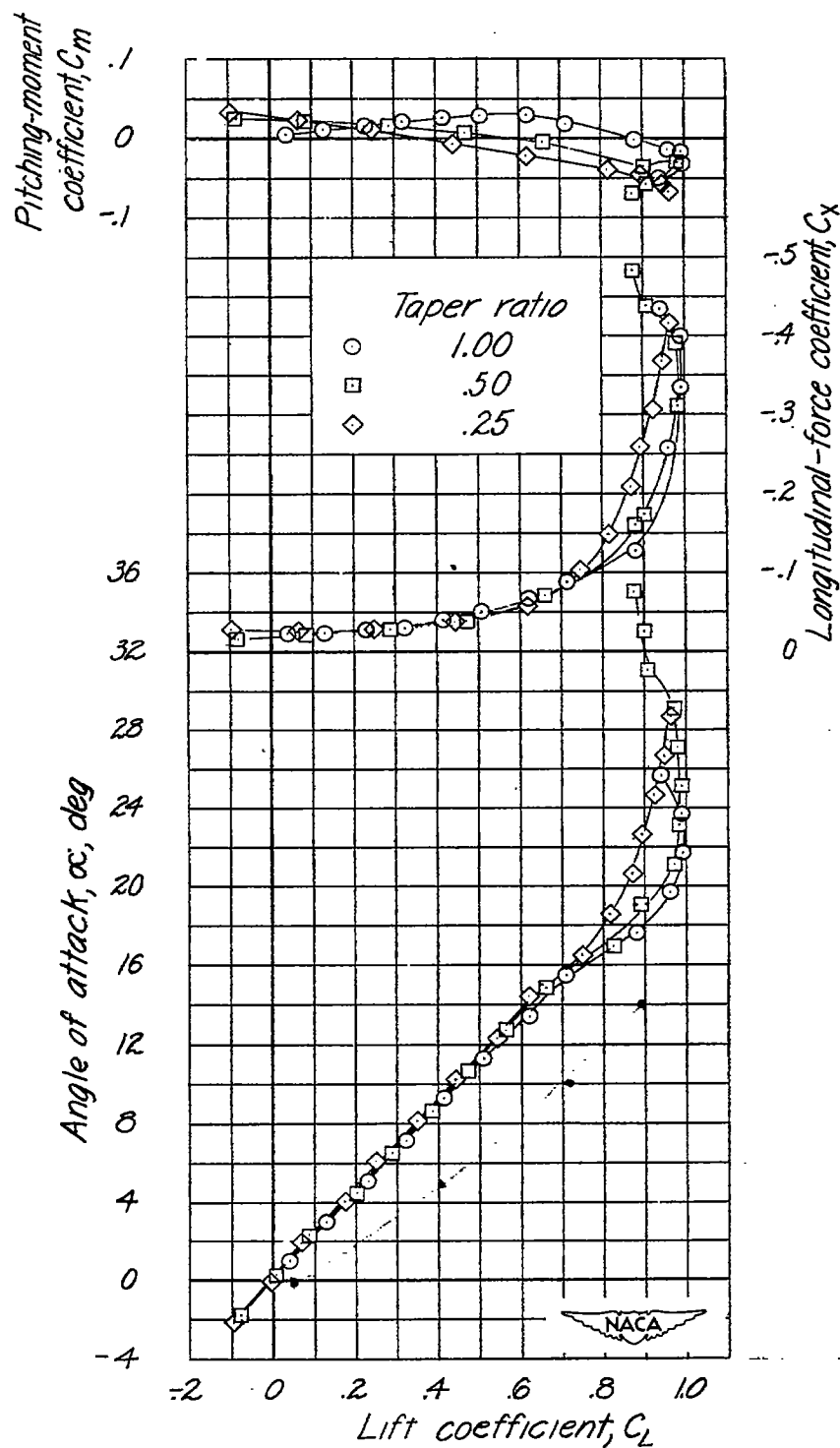


Figure 4.- Variation of longitudinal-force and pitching-moment coefficients and angle of attack with lift coefficient for wings tested.

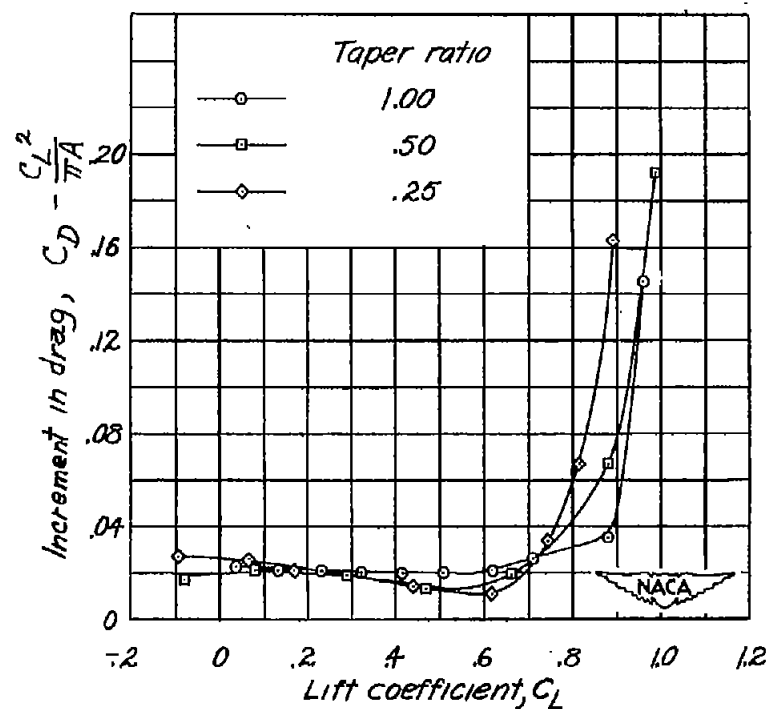


Figure 5.- Variation of increment in drag  $C_D - \frac{C_L^2}{\pi A}$  with lift coefficient for wings tested.

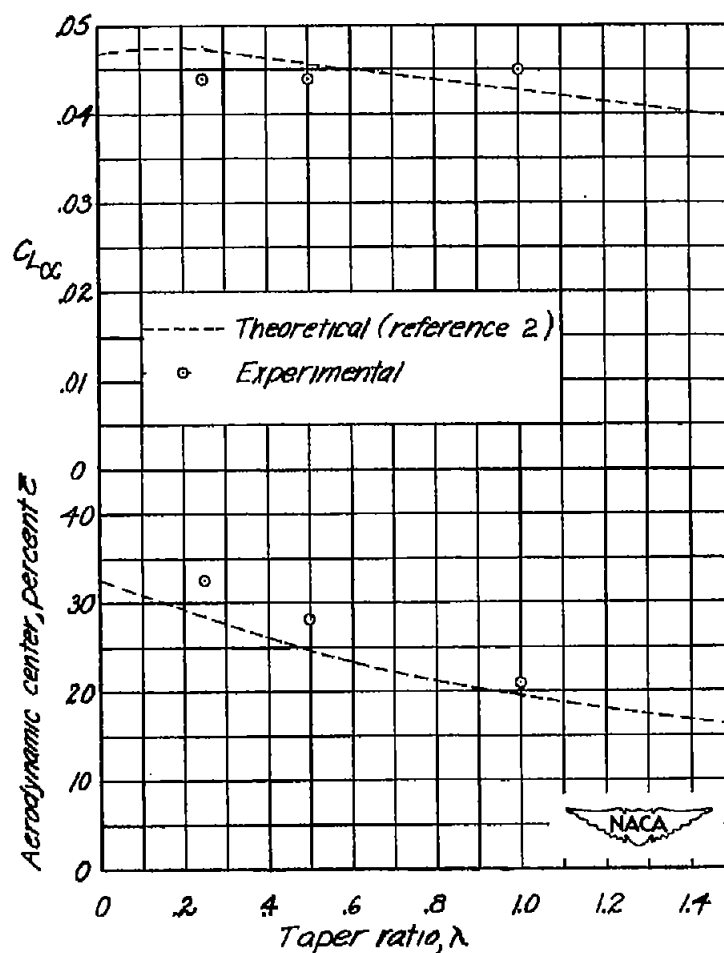


Figure 6.- Comparison of theoretical and experimental variations of  $C_{L\alpha}$  and position of aerodynamic center with taper ratio for wings tested.  $C_L < 0.6$ .



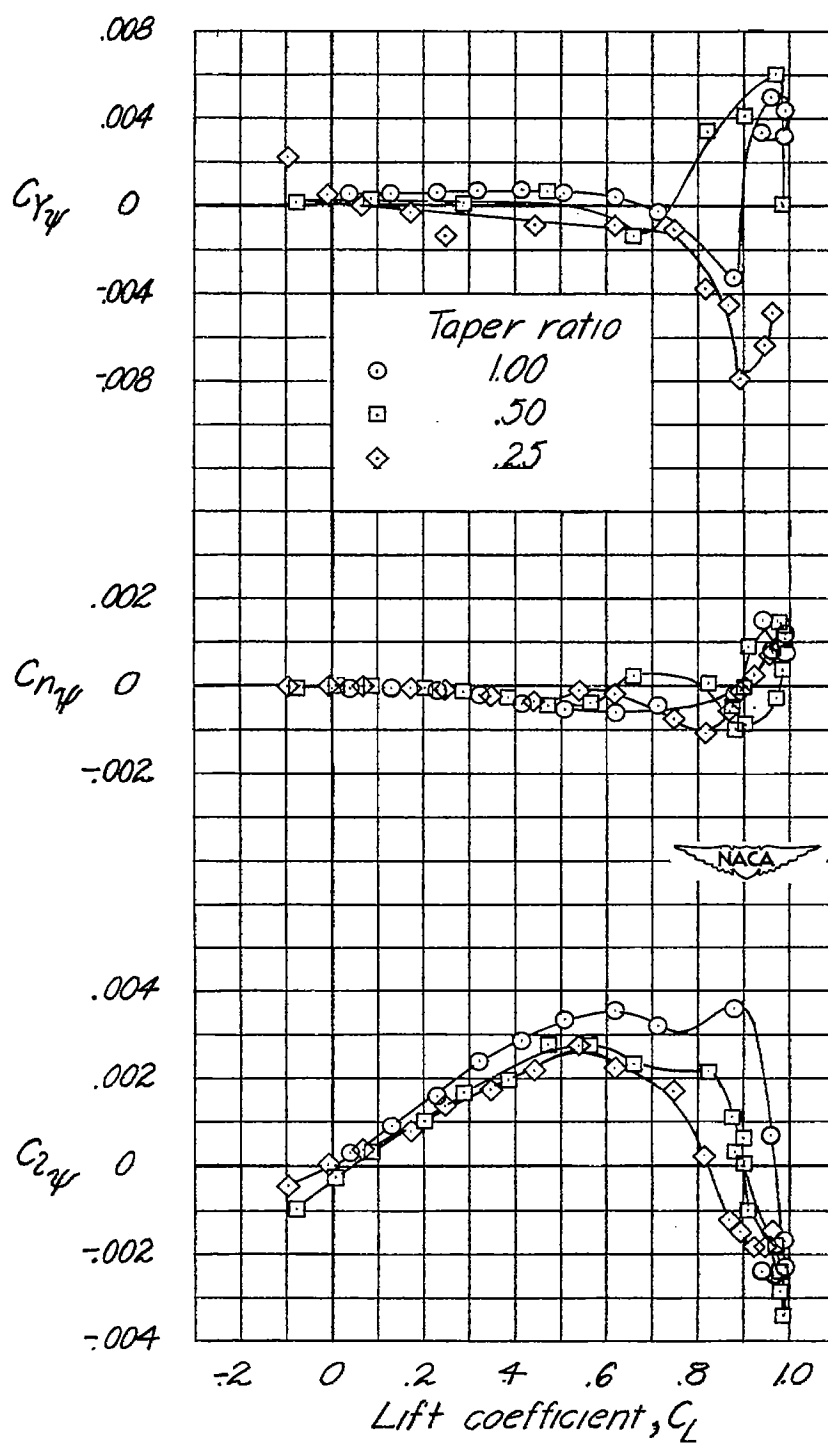


Figure 7.- Variation of  $C_{Y\psi}$ ,  $C_{n\psi}$ , and  $C_{z\psi}$  with lift coefficient for wings tested.

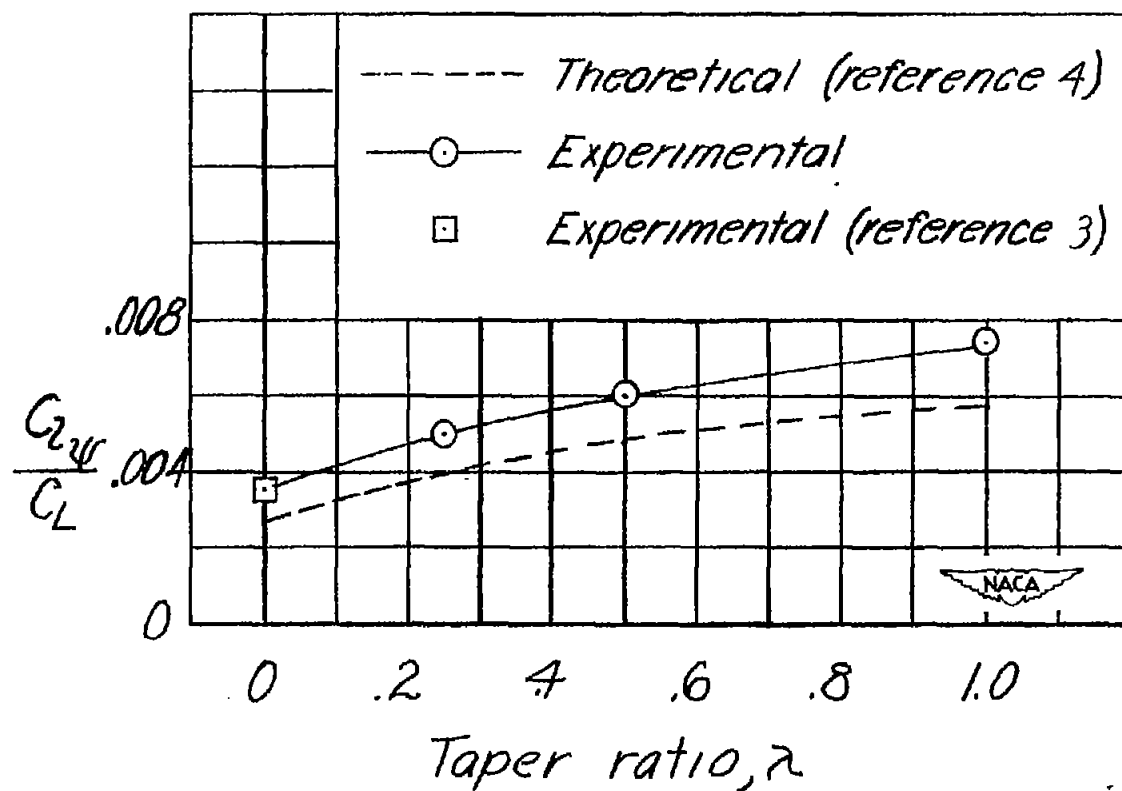


Figure 8.- Comparison of experimental and theoretical variation of  $C_{Di}/C_L$  with taper ratio.  $C_L < 0.6$ .

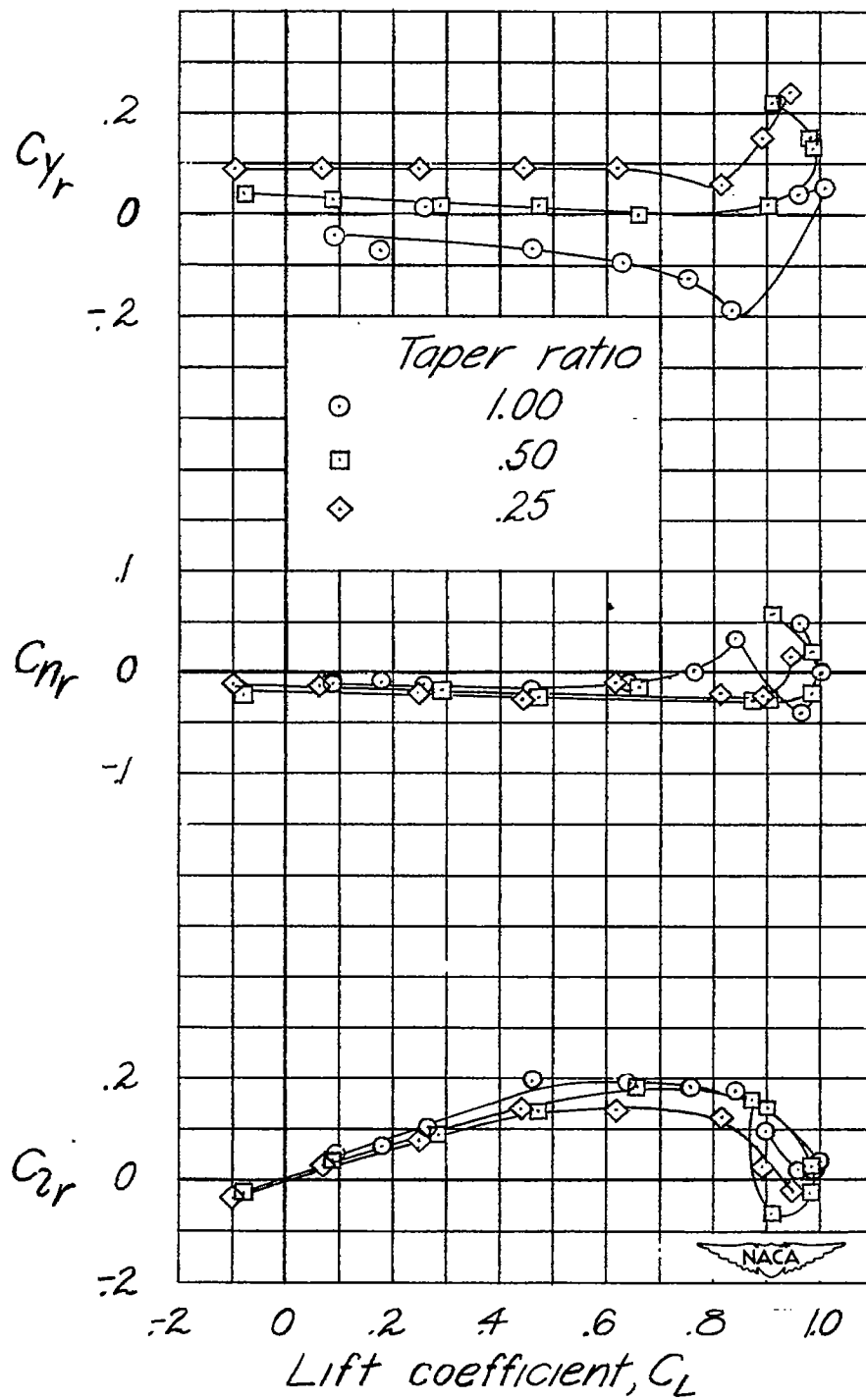


Figure 9.- Variation of  $C_{Yr}$ ,  $C_{nr}$ , and  $C_{lr}$  with lift coefficient for wings tested.  $\psi = 0^\circ$ .

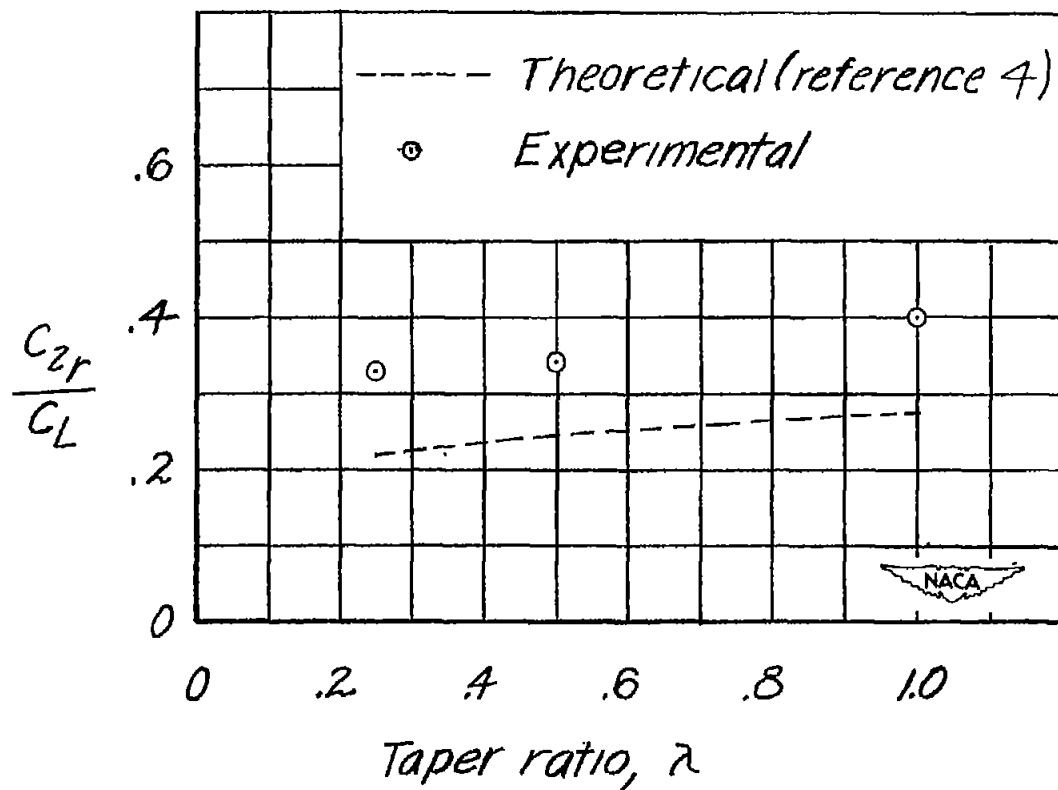


Figure 10.- Comparison of theoretical and experimental variation of  $\frac{C_{zr}}{C_L}$  with taper ratio for wings tested.  $\psi = 0^\circ$ ;  $C_L < 0.6$ .

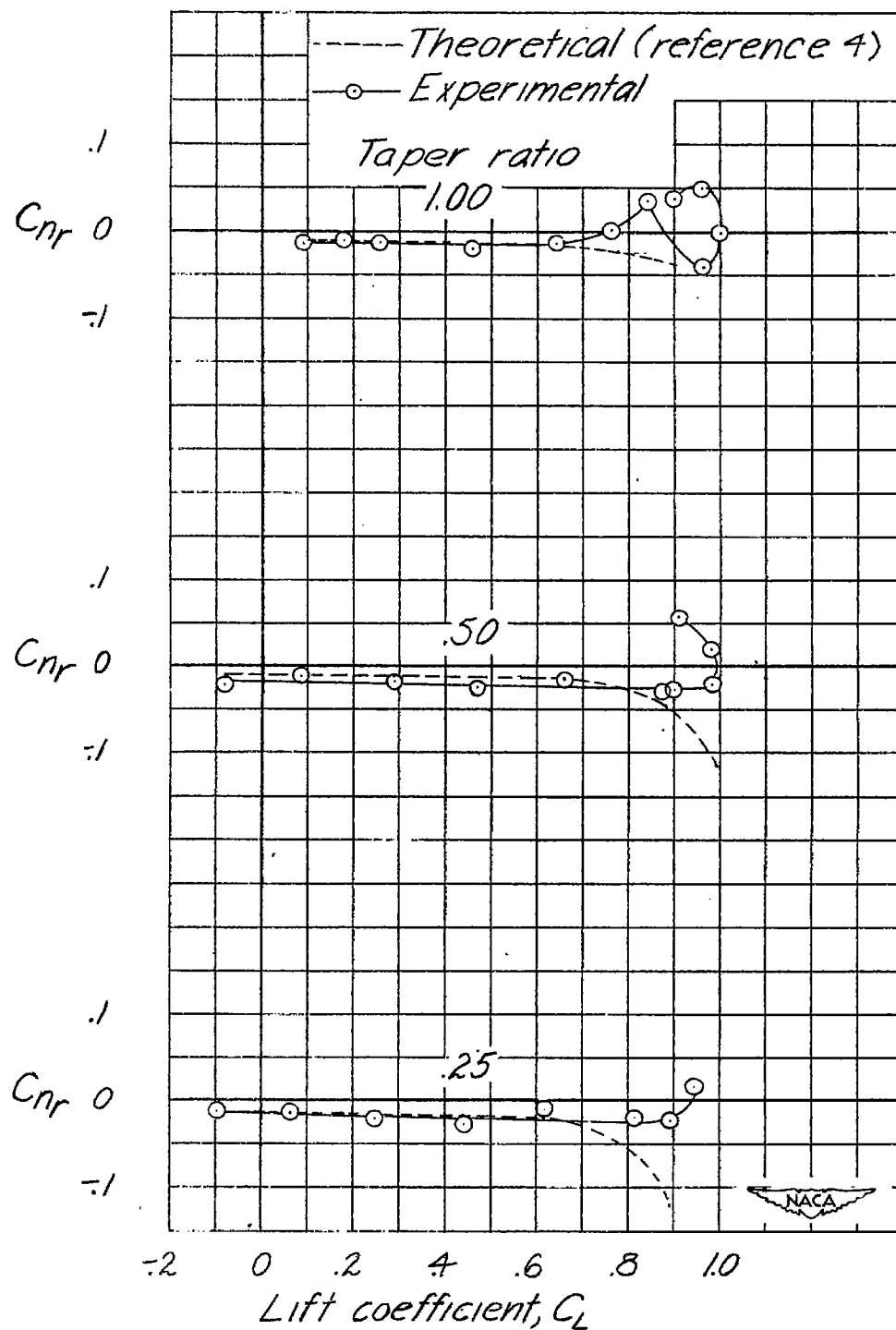


Figure 11.- Comparison of experimental and theoretical variation of  $C_{nr}$  with lift coefficient for wings tested.  $\psi = 0^\circ$ .